Available online at www.sciencedirect.com
ScienceDirect
Journal of Physics and Chemistry of Solids 68 (2007) 1583–1590
JOURNAL OF PHYSICS AND CHEMISTRY OF SOLIDS
www.elsevier.com/locate/jpcs

Hydrothermal synthesis and characterization of nanocrystalline Zn–Mn spinel

Xiang-Dong Zhang[a,b], Zhong-Shuai Wu[b], Jian Zang[b], Da Li[a], Zhi-Dong Zhang[a,*]

[a]*Shenyang National Laboratory for Materials Science, Institute of Metal Research and International Center for Materials Physica, Chinese Academy of Sciences, 72 Wenhua Road, Shenyang 110016, China*
[b]*Department of Chemistry, Liaoning University, Chongshan Road, Shenyang 110036, China*

Received 7 March 2006; received in revised form 26 February 2007; accepted 24 March 2007

Abstract

Hydrothermal method had been used to successfully synthesize the nanocrystalline spinel zinc manganese oxide ($ZnMn_2O_4$) directly from $Zn(CH_3COO)_2 \cdot 2H_2O$, NaOH, $Mn(NO_3)_2$ and H_2O_2 at 170 °C for the reaction time of 48 h. The effects of the synthesis conditions, such as the Zn/Mn molar ratio, the reaction temperature, the reaction time, the zinc source and the concentrations of NaOH and H_2O_2, on the formation of the Zn–Mn spinel were investigated. The products were characterized by means of X-ray diffraction (XRD), inductively coupled plasma-atomic emission spectroscopy (ICP-AES). The results indicated that the compositions of the Zn–Mn spinel with the tetragonal structure were $Zn_{1.14}Mn_{1.86}O_4$. Scanning electron microscope (SEM) and transmission electron microscopy (TEM) images showed that the products at 170 °C were with square-shaped nanocrystalline spinel with the particle size of about 20–50 nm. The thermal behaviors of the products were investigated by thermogravimetric analysis (TG).

Keywords: A. Nanostructures; A. Non-crystalline materials; A. Oxides; B. Chemical synthesis; C. X-ray diffraction

1. Introduction

Zinc manganese oxide ($ZnMn_2O_4$) was one of the important mixed transition-metal oxides with spinel structure [1–8]. It was well known that zinc manganese oxide spinel is a promising technological material for the negative temperature coefficient (NTC) thermistors [5], or the cathode material of the secondary batteries [9] due to their excellent electrochemical properties. Their potential applications were also realized in preparing high-temperature materials [5] and catalyst [10], owing to their high thermal stability of the spinel phase of zinc manganese oxide, and even the precursor for the preparation of porous materials [1–4,8,11,12]. Therefore, many studies had been focused on the synthesis and applications of $ZnMn_2O_4$. So far, zinc manganese oxide spinels had been prepared by solid state reaction [6,13–15], sol–gel [16,17] method, coprecipitation [5,18] or thermal decomposition in air of oxalate precursors [5]. Among these methods, the solid state reaction [6,13–15] was the most conventional method to prepare zinc manganese oxide spinel from zinc oxide (ZnO) and manganese oxides. The products with a good and fine crystalline structure were usually obtained at the temperature between 600 and 1100 °C under a long reaction time. But the solid reaction method had some disadvantages such as large particle size, broad particle size distribution and high reaction temperature.

The hydrothermal method was a relatively mild and powerful method to prepare nanocrystalline materials. In this paper, the hydrothermal method was used to synthesize the nanocrystalline spinel of zinc manganese oxide ($ZnMn_2O_4$). The hydrothermal synthesis reaction was realized from the mixing of $Zn(CH_3COO)_2 \cdot 2H_2O$, NaOH, $Mn(NO_3)_2$ and H_2O_2 at 170 °C for the reaction time of 48 h.

*Corresponding author.
E-mail address: xd623@sina.com (Z.-D. Zhang).

0022-3697/$ - see front matter © 2007 Elsevier Ltd. All rights reserved.
doi:10.1016/j.jpcs.2007.03.044

2. Experimental

2.1. Synthesis of spinel zinc manganese oxide

A mixed solution of 0.92 ml H_2O_2 (3%) and 6 ml NaOH (0.6 M) was poured slowly into a Teflon-lined stainless-steel autoclave filled with 3 ml $Mn(NO_3)_2$ (0.3 M) while stirring vigorously, and the reaction solution was continually stirred and kept for 0.5 h at the room temperature. Then, the dihydrate acetate zinc ($Zn(CH_3COO)_2 \cdot 2H_2O$) in the Zn/Mn molar ratio ranging from 0 to 1.0 (0, 0.2, 0.4, 0.5, 0.55, 0.6, 0.65, 0.7, 0.75, 0.8, 0.9 and 1.0, respectively) was added into the reaction solution. After this the reaction solutions were hydrothermally treated under autogenous pressure to obtain hydrothermally treated samples. The reaction temperature was set between 150 and 190 °C and hydrothermal time between 0 and 118 h. The samples prepared hydrothermally were cooled naturally, then the precipitates were filtered and washed with distilled water several times until pH = 7, and finally air-dried at room temperature.

All the chemical reagents used in the experiment were A.R. grade and used without further purification and treatment.

2.2. Characterization

Powder X-ray diffraction (XRD) analysis was carried out to identify the phase of the samples by using a Bruker D8 X-ray diffractometer with Cu Kα radiation ($\lambda = 1.540600$ Å) monochromated by graphite at 40 kV and 40 mA. The chemical composition was determined by using inductively coupled plasma (ICP; Nippon Jarrel Ash, ICAP575II) after the samples were dissolved in the solution of HNO_3 and H_2O_2. Thermogravimetric analysis (TG–DTA) was performed in air by a Mettler TGA/SDTA851e with a heating rate of 10 °C min^{-1}. The morphologies of the samples were observed by the scanning electron microscopy (SEM; S-570F) and the transmission electron microscopy (TEM; JEX-100SX).

3. Results and discussion

3.1. The ratio of zinc to manganese

As shown in Fig. 1, spinel zinc manganese oxide ($ZnMn_2O_4$) could be hydrothermally synthesized directly from $Zn(CH_3COO)_2 \cdot 2H_2O$, NaOH, $Mn(NO_3)_2$ and H_2O_2 at 170 °C for 48 h with a certain ratio of Zn/Mn. The single-phase spinel with tetragonal structure could only be obtained in a specified Zn/Mn ratio ranging between 0.55 and 0.6 (see Fig. 1e, f). Outside of this range, some other species were formed. The XRD patterns in Fig. 1 clearly showed the effects of Zn/Mn ratio on the process of the transformation of birnessite phase into the single-phase tetragonal $ZnMn_2O_4$. Birnessite (JCPDS23-1046) had firstly been hydrothermally formed from the precursor

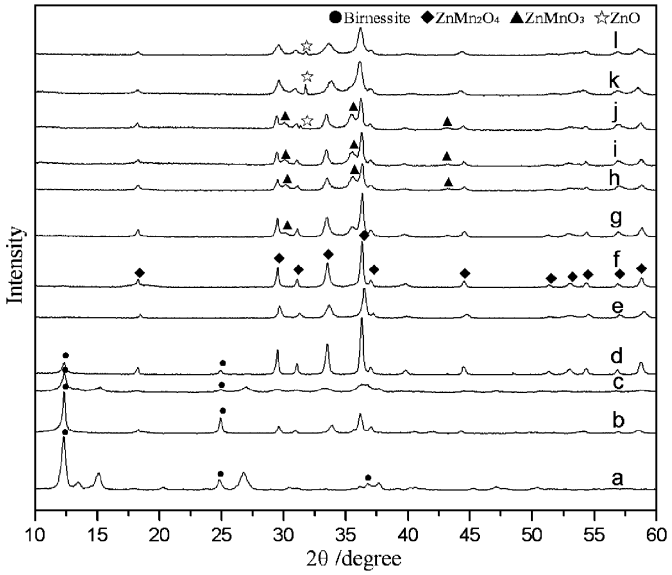

Fig. 1. XRD patterns of the samples obtained hydrothermally at 170 °C for 48 h at different Zn/Mn ratios of (a) 0, (b) 0.2, (c) 0.4, (d) 0.5, (e) 0.55, (f) 0.6, (g) 0.65, (h) 0.7, (i) 0.75, (j) 0.8, (k) 0.9 and (l) 1.0.

β-MnOOH while stirring vigorously at room temperature. During the hydrothermal condition, the β-MnOOH was transformed into γ-MnOOH (JCPDS24-0713) whose characteristic peaks are at 2θ of 26.68°, 15.2°, and then γ-MnOOH was partly transformed into birnessite without $Zn(CH_3COO)_2 \cdot 2H_2O$ added to the precursor β-MnOOH (Fig. 1a). The intensities of the birnessite peak at 2θ of 12.40°, 25.00° and 36.60° gradually decreased with the increase of the Zn/Mn ratio from 0 to 0.4 (see Fig. 1a–d). At the same time, the intensities of the tetragonal spinel peaks at 2θ of 36.28°, 33.52°, 29.52°, 18.24° and 31.08° increased. When the ratio of Zn/Mn reached 0.55, the peak of birnessite phase finally disappeared and all peaks were due to tetragonal spinel of $ZnMn_2O_4$ (JCPDS24-1133, Fig. 1e, f). Then, the single-phase spinel $ZnMn_2O_4$ was formed when the ratio of Zn/Mn was 0.6 (Fig. 1f). ICP-AES result showed that the chemical composition of the compound was $Zn_{1.14}Mn_{1.86}O_4$ at this point. The cubic $ZnMnO_3$ phase (Fig. 1g, j) or ZnO phase (JCPDS36-1451, Fig. 1k, l) together with the tetragonal spinel was precipitated when the ratio of Zn/Mn was larger than 0.6. This result indicated that the competitive reaction between the tetragonal spinel phase and cubic $ZnMnO_3$ or ZnO phase existed in the process of the formation of tetragonal phase. The formation of cubic $ZnMnO_3$ or ZnO might result from the surplus of Zn^{2+}.

The morphologies of the as-prepared products were observed by TEM (Fig. 2). It was found that the nanocrystalline $ZnMn_2O_4$ with square-shaped particle was obtained at 170 °C for 48 h. Fig. 2 shows the TEM images with the low magnification (a, c, f) and high magnification (b, d, g, e) for the samples obtained at the Zn/Mn ratio of 0.55, 0.6 and 0.65, respectively. TEM images (a, c, f) indicated that the particle distribution in the

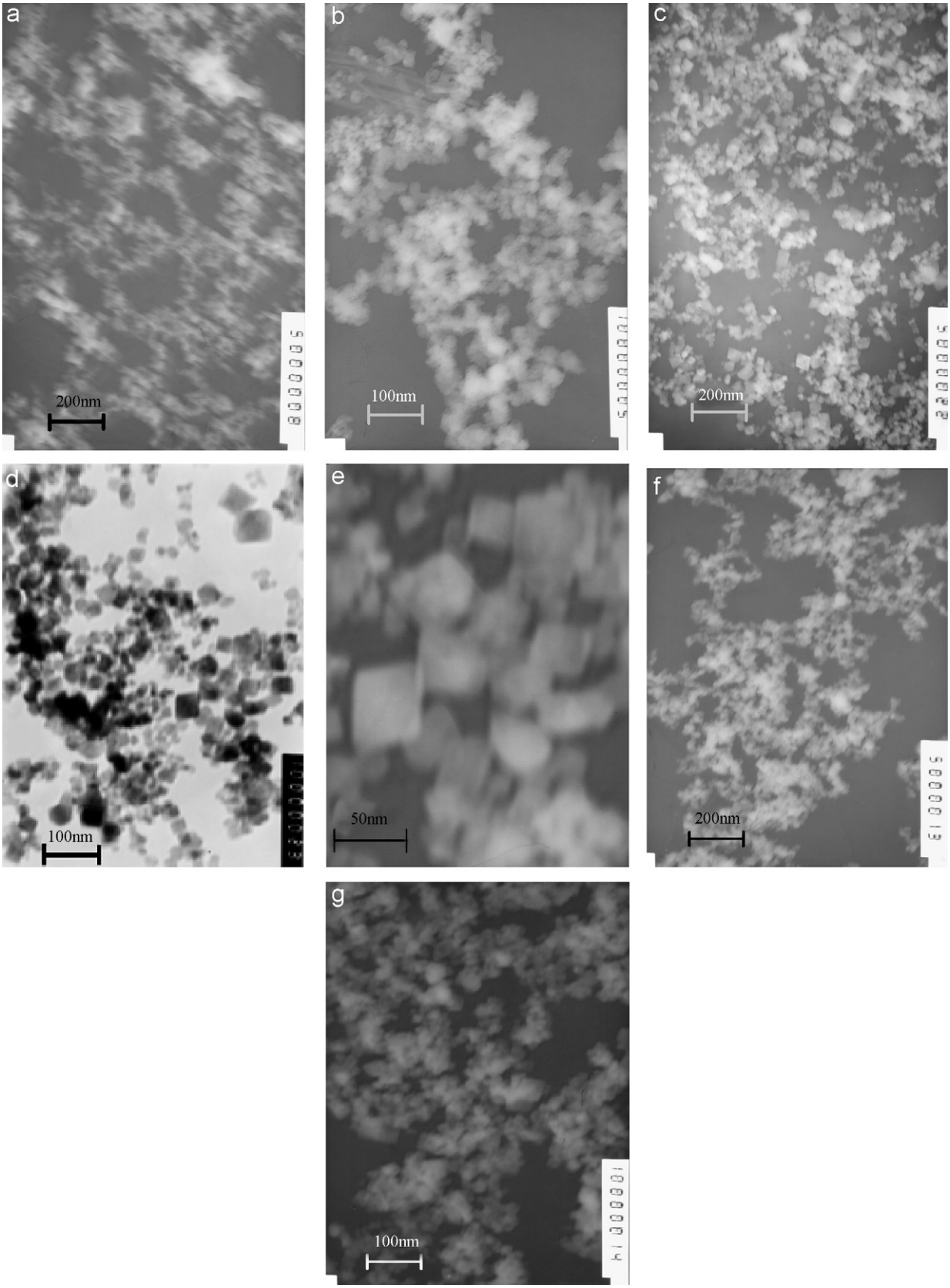

Fig. 2. Low and high-magnification TEM images of the samples obtained hydrothermally at 170 °C with the Zn/Mn ratios of 0.55 (a, b), 0.6 (c, d, e) and 0.65 (f, g), respectively.

samples observed at the Zn/Mn ratio of 0.6 was more uniform than one in the samples at the Zn/Mn ratios of 0.55 or 0.65. The mean size of particles was between 10 and 60 nm where some spherical particles were aggregated by the square shape of nanoparticles (Fig. 2b, d, g). High-magnification image further revealed the nanoparticles were square-shaped with the mean size between 30 and 40 nm at the Zn/Mn ratio of 0.6.

3.2. Effects of reaction temperature

Fig. 3 shows the XRD patterns of the samples obtained hydrothermally for 48 h at 150, 170 and 190°C, respectively, where the ratio of Zn/Mn was 0.6. As shown in Fig. 3, the sample obtained at 150 °C consisted of the mixed phases of birnessite and tetragonal spinel (Fig. 3a), while the primary phase prepared at 190 °C was the γ-MnOOH phase (Fig. 3c). The SEM image of this sample in Fig. 4 shows that the particles were of the strip-like structure that was a typical morphology of γ-MnOOH. Only at 170 °C the single phase of spinel $ZnMn_2O_4$ was prepared (Fig. 3b). This result indicated that the relatively high temperature of 190 °C was able to accelerate the transformation of the precursor β-MnOOH into γ-MnOOH (Fig. 3c), and the comparatively low temperature of 150 °C was unable to fully make this transformation and further the conversion of β-MnOOH to birnessite (Fig. 3a).

3.3. Effects of reaction time

Fig. 5 shows the XRD patterns of the samples prepared hydrothermally at 170 °C in various reaction times from 0 to 72 h. The powder XRD results clearly showed that hydrothermal reaction time was an important influencing factor for the formation of tetragonal spinel $ZnMn_2O_4$. As

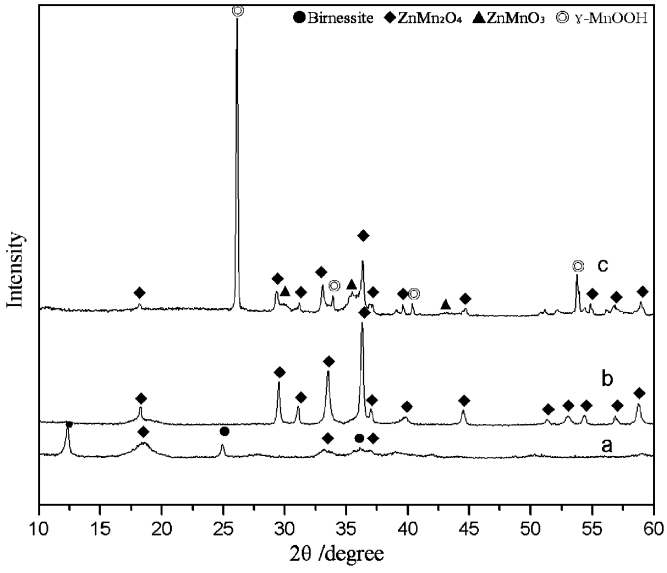

Fig. 3. XRD patterns of the samples obtained hydrothermally at (a) 150 °C, (b) 170 °C and (c) 190 °C for 48 h at the Zn/Mn ratio of 0.6.

Fig. 4. SEM image of the sample obtained hydrothermally at 190 °C for 48 h at the Zn/Mn ratio of 0.6.

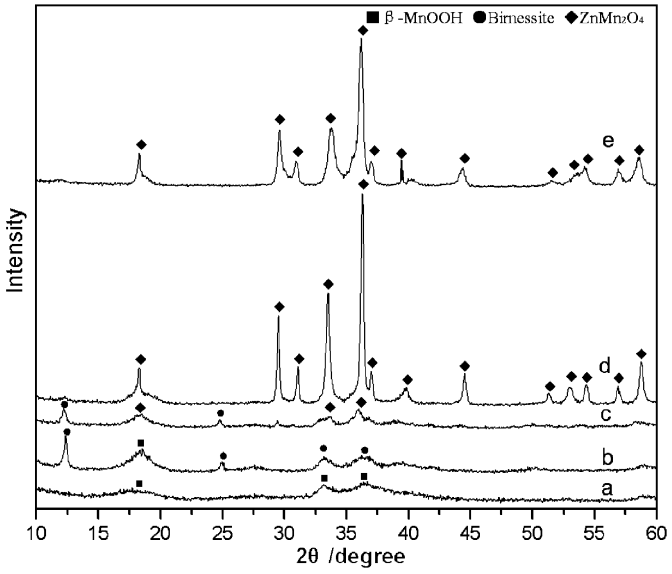

Fig. 5. XRD patterns of the samples obtained hydrothermally at the Zn/Mn ratio of 0.6 at 170 °C for the reaction time of (a) 0 h, (b) 12 h, (c) 24 h, (d) 48 h and (e) 72 h, respectively.

the diffraction peaks at 2θ of 19.5°, 33.26° and 37.78° in Fig. 5a were due to β-MnOOH (JCPDS18-0804), the β-MnOOH phase had been formed before the hydrothermal treatment. With increasing hydrothermal reaction time up to 12 h (Fig. 5b), the β-MnOOH phase was partly oxidized to form the Na-birnessite or Zn-birnessite accompanied the insertion of Na^+ into the interlayer space. The peaks of β-MnOOH and birnessite phases started decreasing or disappearing (see Fig. 5c) when the reaction time was extended to 24 h. Until the reaction time reached 48 h, the single phase of the tetragonal spinel of $ZnMn_2O_4$ (JCPDS24-1133, Fig. 5d) was obtained. However, if the reaction time was further extended to 72 h, the diffraction peaks of the tetragonal spinel appearing in the XRD pattern of the sample (Fig. 5e) were gradually weaker

and broader, which indicated that the size of nanocrystalline would make for the smaller nanoparticles.

3.4. Effect of zinc source

Fig. 6 shows that the XRD patterns of the samples obtained hydrothermally at 170 °C for 48 h at the Zn/Mn ratio of 0.6 when the zinc source was (a) $Zn(CH_3COO)_2 \cdot 2H_2O$, (b) $ZnSO_4 \cdot 7H_2O$ and (c) $ZnCl_2$. The sample obtained by using $Zn(CH_3COO)_2 \cdot 2H_2O$ (Fig. 6a) as zinc source was with the single phase of tetragonal spinel $ZnMn_2O_4$. The other two samples obtained by using $ZnCl_2$ (Fig. 6b) or $ZnSO_4 \cdot 7H_2O$ (Fig. 6c) as zinc sources were with the mixed phases of birnessite and spinel. The XRD results suggested that the existence of $C_2H_5O^{2-}$was more favorable of formation of birnessite than the existence of SO_4^{2-} or Cl^-. The formation speed of birnessite at the initial stage might directly influence the following transformation of birnessite into spinel. These results also agreed with the previous report [19] where Luo and Suib discussed the effect of anion on the formation of birnessite and found that the existence of $C_2H_5O^{2-}$ could accelerate to form birnessite in a fast crystallization period. From the results, the effect on the formation of birnessite could been ranked as: $C_2H_5O^{2-} > SO_4^{2-} > Cl^-$.

3.5. Effect of the concentrations of H_2O_2 and NaOH

In order to investigate the effects of products with the quantity of NaOH (0.6 M) and H_2O_2 (3%), the quantity of NaOH was chosen to be 5 ml, and the quantity of H_2O_2 was chosen to be 1.2 ml, while the reaction was held under same condition at 170 °C for the reaction time of 48 h at the Zn/Mn ratio of 0.6 by using $Zn(CH_3COO)_2 \cdot 2H_2O$ as zinc source. As the quantity of NaOH was reduced to 5 ml, it was found that a lot of ZnO phase (at 2θ of 31.72°, 33.88°) was formed because of the lack of NaOH leading to the surplus of Zn^{2+}, and accompanied partly the formation of γ-MnOOH and tetragonal spinel (see Fig. 7a). When the quantity of H_2O_2 added was 1.2 ml, the phase of the cubic $ZnMnO_3$ product appeared besides tetragonal spinel $ZnMn_2O_4$ (Fig. 7b). Because the Mn^{3+} ions in the spinel $ZnMn_2O_4$ were oxidized by the surplus of H_2O_2, together

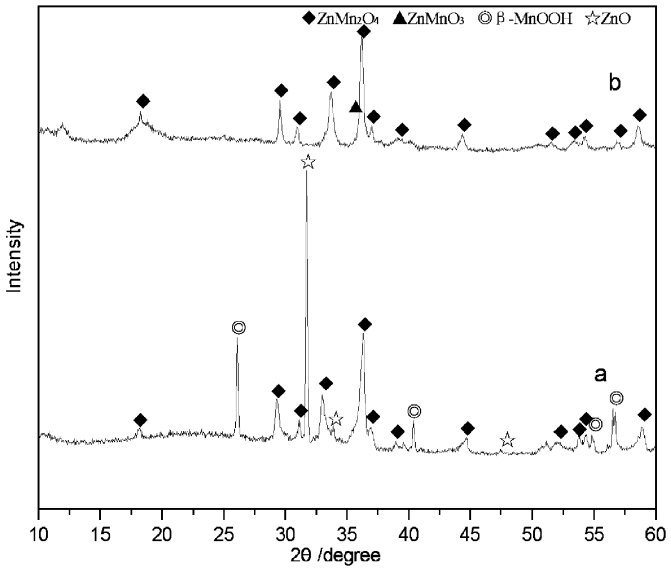

Fig. 7. XRD patterns of the samples obtained hydrothermally at 170 °C for 48 h from (a) 5 ml NaOH and 0.92 ml H_2O_2 and (b) 6 ml NaOH and 1.2 ml H_2O_2 at the Zn/Mn ratio of 0.6.

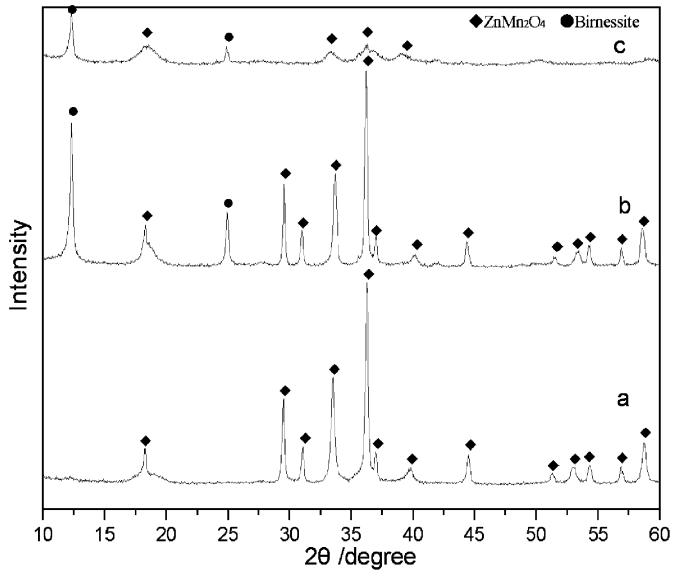

Fig. 6. XRD patterns of the samples obtained hydrothermally at 170 °C for 48 h at the Zn/Mn ratio of 0.6 with different zinc sources: (a) $Zn(CH_3COO)_2 \cdot 2H_2O$, (b) $ZnSO_4 \cdot 7H_2O$ and (c) $ZnCl_2$.

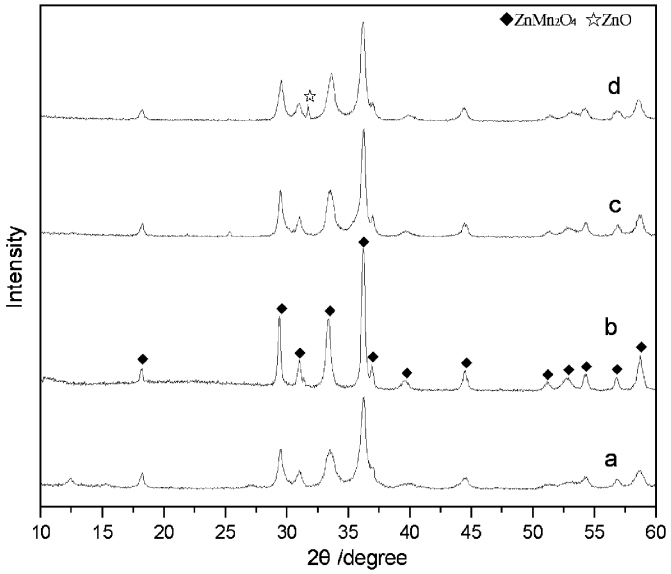

Fig. 8. XRD patterns of the samples obtained hydrothermally at 170 °C for 72 h at the Zn/Mn ratio of (a) 0.5, (b) 0.6, (c) 0.8 and (d) 1.0, respectively.

with the J–T effect of the Mn^{3+} ions [1–4], this led to the transition from tetragonal spinel into cubic $ZnMnO_3$.

3.6. Effect of extending hydrothermal reaction time with various Zn/Mn ratios

Fig. 8 shows the XRD patterns of the samples synthesized hydrothermally at 170 °C for a longer reaction time of 72 h with various Zn/Mn ratios of (a) 0.5, (b) 0.6, (c) 0.8 and (d) 1.0. Compared to the XRD pattern in Fig. 1d, the diffraction peaks of birnessite in Fig. 8a with longer reaction time almost disappeared except that the only little and weak peak was at 2θ of 12.46°. However, the single phase of spinel $ZnMn_2O_4$ was again synthesized at 170 °C when the ratio of Zn/Mn was 0.8 under hydrothermal reaction time of 72 h. In contrast to the XRD pattern of the sample obtained at the reaction time of 48 h (Fig. 1j), the cubic $ZnMnO_3$ was disappeared and transformed into the spinel $ZnMn_2O_4$. Note that the XRD patterns of the samples obtained at the Zn/Mn ratio of 0.6 (Fig. 8b) and 1.0 (Fig. 8d) with the treatment time of 72 h were almost no difference to ones with the treatment

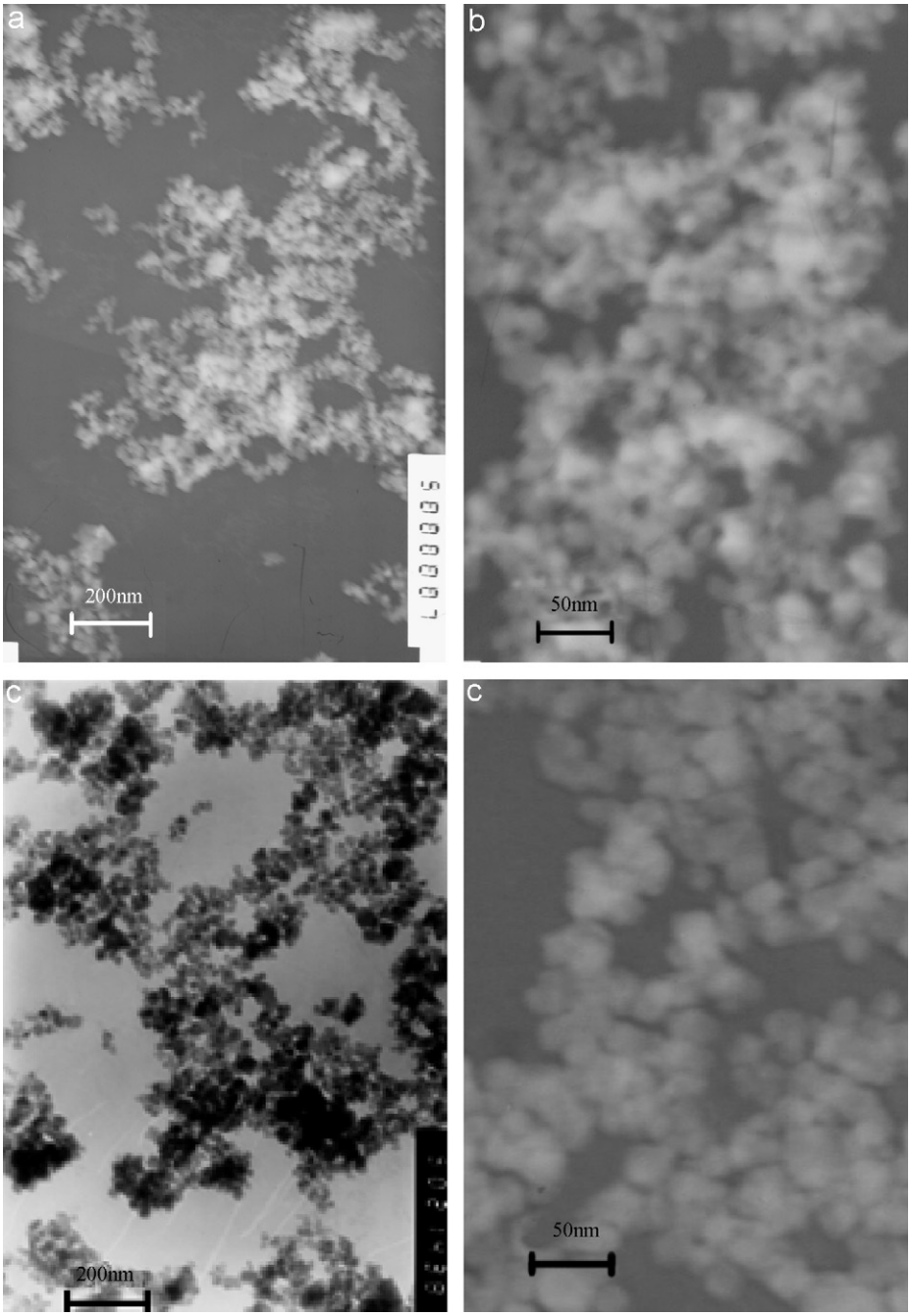

Fig. 9. Low and high-magnification TEM images of the samples obtained hydrothermally at 170 °C for 118 h at the Zn/Mn ratio of 0.55 (a, b) and 0.65 (c, d), respectively.

time of 48 h (Fig. 1f, l). The results indicated that extending hydrothermal reaction time was favorable for the formation of the spinel $ZnMn_2O_4$. This was further supported by the TEM images of the tetragonal $ZnMn_2O_4$ spinel in Fig. 9, where the samples were synthesized hydrothermally at 170 °C for the reaction time of 118 h with the Zn/Mn ratio of 0.55 (a, b) and 0.65 (c, d), respectively. The particle size in Fig. 9 was smaller than the one obtained at 170 °C for the reaction time of 48 h (see Fig. 2).

3.7. Thermal analysis of Zn–Mn spinel

In order to investigate the thermal stability, the thermogravimetric (TG) analysis was carried out. Fig. 10 shows the TG curves of the as-prepared $ZnMn_2O_4$ obtained at 170 °C for 48 h while the Zn/Mn ratio was 0.55 (a) and 0.6 (b), respectively. There were three weight losses occurring either in the regions of 30–110 °C, 110–486 °C and 574–646 °C in Fig. 10a or in the regions of 30–108 °C, 110–466 °C and 578–648 °C in Fig. 10b. There was one weight increase in the region of either 486–574 °C in Fig. 10a or 466–578 °C in Fig. 10b. The little weight loss below 110 °C could be ascribed to the evaporation of the absorbed water in the air. The second weight loss in the regions of either 110–486 °C (a) or 466 °C (b) corresponded to the loss 1.99% (a) or 1.56% (b) of the oxygen excess δ in $Zn_xMn_{3-x}O_{4+\delta}$ [5,7]. This result agreed with that the nonstoichiometric coefficient δ diminished as the zinc content increased [5]. The process of weight increase in either the range 486–574 °C (a) or 466–578 °C (b) was attributed to the oxidation of the tetrahedral Mn^{2+} cations in the spinel phase, which gave rise to α-Mn_2O_3 [5]. The weight losses of about 0.05% in either 574–646 °C (a) or 0.06% in 578–648 °C (b) should correspond to the reduction of the Mn^{3+}, which led to the oxygen loss. As a matter of fact that the weight loss in the whole temperature range was only either 2.61% (a) or 2.21% (b), the spinel phase $ZnMn_2O_4$ with a tetragonal structure obtained hydrothermally in this paper had a high thermal stability, identical to the results in the literature [1,3,7] reported by Driessens et al.

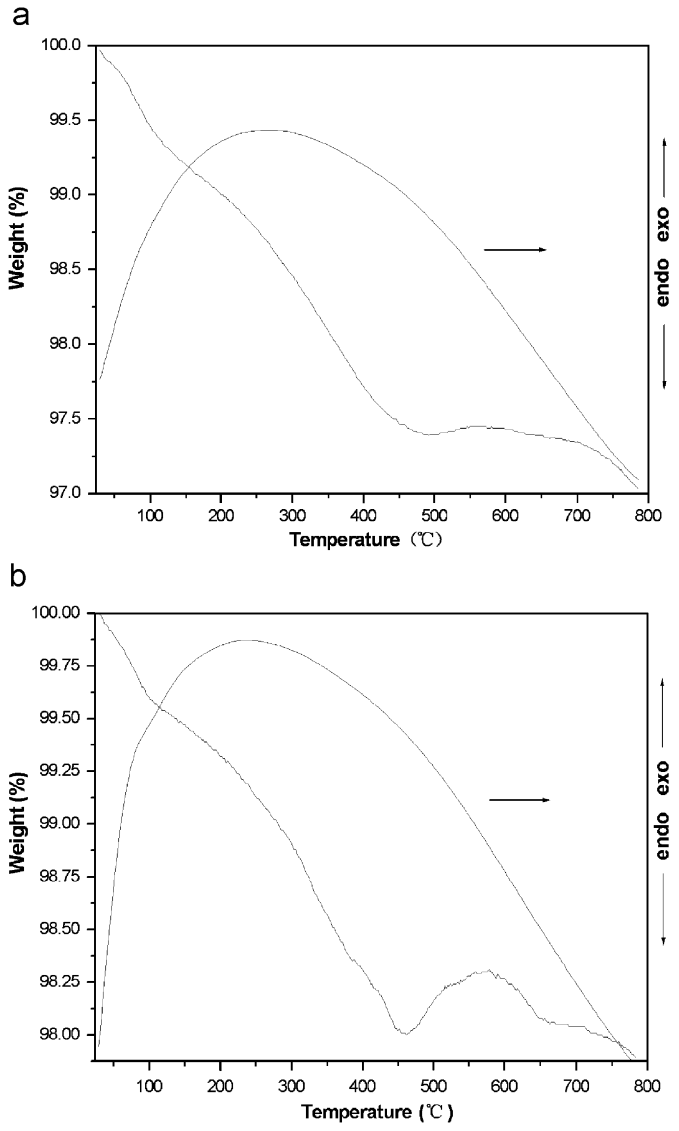

Fig. 10. TG curve of the sample obtained hydrothermally at 170 °C for 48 h at the Zn/Mn ratio of (a) 0.55 and (b) 0.6, respectively.

4. Conclusions

The nanocrystalline spinel $ZnMn_2O_4$ with the particle size of about 50 nm has been successfully synthesized by a mild hydrothermal method directly from $Zn(CH_3COO)_2 \cdot 2H_2O$, NaOH, $Mn(NO_3)_2$ and H_2O_2 at 170 °C. The synthesis process of the spinel $ZnMn_2O_4$ was dependent on the Zn/Mn molar ratio, hydrothermal temperature, reaction time, zinc source, as well as the concentrations of NaOH and H_2O_2 in the starting solution. Effects of above synthesis parameters on the formation of spinel $ZnMn_2O_4$ were investigated. The sample obtained by hydrothermal method had shown a high thermal stability. Compared to the conventional methods to prepare zinc manganese oxide spinel, the hydrothermal method was believed to be a cheap and technically matured method for preparing nanocrystalline $ZnMn_2O_4$.

Acknowledgments

This work has been supported by the National Natural Science Foundation of China under Grant No. 50332020 and the Natural Science Foundation of Liaoning Province.

References

[1] M. Rosenberg, P. Nicolau, R. Manaila, et al., J. Phys. Chem. Solids 24 (1963) 1419.
[2] J.D. Dunitz, L.E. Orgel, J. Phys. Chem. Solids 3 (1957) 20.
[3] K.S. Irani, A.P.B. Sinaha, A.B. Biswas, J. Phys. Chem. Solids 17 (1960) 101.
[4] M. O'Keeffe, J. Phys. Chem. Solids 21 (1961) 172.
[5] S. Guillemet-Fritsch, C. Chanel, J. Sarrias, S. Bayonne, A. Rousset, X. Alcobe, M.L. Martinez Sarrion, Solid State Ionics 128 (2000) 233.

[6] S. Asbrink, A. Waskowska, L. Gerward, J. Staun Olsen, E. Talik, Phys. Rev. B 60 (1999) 12651.
[7] F.C.M. Driessens, G.D. Rieck, J. Inorg. Nucl. Chem. 26 (1964) 1593.
[8] A.P.B. Sina, N.R. Sanjana, A.B. Biswas, Acta Crystallogr. 10 (1957) 439.
[9] H. Yang, H.Q. Yang, Y.L. Lu, N. Li, B.X. Li, J. Power Sources 62 (1996) 223.
[10] G. Fierro, M.Lo. Jacono, M. Inversi, R. Dragone, G. Ferraris, Appl. Catal. B: Environ. 30 (2001) 173.
[11] E.S. Toberer, R. Seshadri, Adv. Mater. 17 (2005) 2244.
[12] E.S. Toberer, J.P. Lofvander, R. Seshadri, Chem. Mater. 18 (2006) 1047.
[13] I.O. Troyanchuk, A.I. Akimov, N.V. Kasper, V.V. Mikhailov, Fiz. Tverd. Tela. 36 (1994) 3263.
[14] K. Chhor, J.F. Bocquet, C. Pommier, B. Chardon, J. Chem. Thermodyn. 18 (1986) 89.
[15] J.V. Dubrawski, React. Solids 2 (1987) 315.
[16] G. Monros, J. Carda, M.A. Tena, P. Escribano, J. Badenes, E. Cordoncillo, J. Mater. Chem. 5 (1) (1995) 85.
[17] K.L. Kim, Y.R. Park, J. Crystal Growth 270 (2004) 162.
[18] M. Rosenberg, P. Nicolau, R. Manaila, P. Pausescu, J. Phys. Chem. Solids 24 (1963) 1419.
[19] J. Luo, S.L. Suib, J. Phys. Chem. B 101 (1997) 10403.